Cellular Physiology and Biochemistry

Cell Physiol Biochem 2020;54:15-26
DOI: 10.33594/000000202
Published online: 10 January 2020
Accepted: 10 December 2019

Original Paper

Nanoscale Mapping Reveals Functional Differences in Ion Channels Populating the Membrane of Primary Cilia

Jose V. Torres-Pérez[a] Hanzla Naeem[a] Clare L. Thompson[a] Martin M. Knight[a] Pavel Novak[a,b,c]

[a]School of Engineering and Materials Science, Queen Mary University of London, London, UK, [b]Department of Medicine, Imperial College London, Hammersmith Hospital, London, UK, [c]National University of Science and Technology «MISiS», Moscow, Russia

Key Words
Nanopipette • Primary cilium • Mechanoreceptors • Scanning ion conductance microscopy

Abstract
Background/Aims: The primary cilium is a nanoscale membrane protrusion believed to act as a mechano-chemical sensor in a range of different cell types. Disruptions in its structure and signalling have been linked to a number of medical conditions, referred to as ciliopathies, but remain poorly understood due to lack of techniques capable of investigating signal transduction in cilia at nanoscale. Here we set out to use latest advances in nanopipette technology to address the question of ion channel distribution along the structure of primary cilium. ***Methods:*** We used glass nanopipettes and Scanning Ion Conductance Microscopy (SICM) to image 3D topography of intact primary cilia in inner medullary collecting duct (IMCD) cells with nanoscale resolution. The high-resolution topographical images were then used to navigate the nanopipette along the structure of each cilium and perform spatially resolved single-channel recordings under precisely controlled mechanical and chemical stimulation. ***Results:*** We have successfully obtained first single-channel recordings at specific locations of intact primary cilia. Our experiments revealed significant differences between the populations of channels present at the ciliary base, tip and within extra-ciliary regions in terms of mean conductance and sensitivity to membrane displacement as small as 100 nm. Ion channels at the base of cilium, where mechanical strain is expected to be the highest, appeared particularly sensitive to the mechanical displacement. ***Conclusion:*** Our results suggest the distribution of ion channels in the membrane of primary cilia is non-homogeneous. The relationship between the location and function of ciliary ion channels could be key to understanding signal transduction in primary cilia.

Pavel Novak
and Martin M. Knight

Faculty of Medicine, Imperial College London,
Commonwealth Building, Du Cane Road, London, W12 0NN (United Kingdom)
Tel. +44 (0) 20 3313 2362, E-Mail p.novak@imperial.ac.uk

School of Engineering and Materials Science, Queen Mary University of London,
Engineering Building, Mile End Road, London, E1 4NS (United Kingdom)
Tel. +44 (0)20 7882 8868, E-Mail m.m.knight@qmul.ac.uk

Introduction

The primary cilium is a single immotile antenna-like organelle protruding from the membrane of most mammalian cells that comprises a distinct cellular compartment with a specific population of ion channels and receptors [1–4]. Although initially considered as an evolutionary vestigial structure, the primary cilium has been suggested to play a role in a number of physiological processes [5–7]. Defects in cilia formation or function are implicated in a great variety of human pathologies, termed ciliopathies, such as polycystic kidney disease (PKD) [1, 8, 9]. Primary cilia display specific ultrastructure [7, 10, 11] and play a key role in the cellular response to chemical and mechanical alterations, serving as sensory platforms to flow, compression and pressure [2, 5, 6, 12]. Various proteins such as polycystin-1 (PC1), polycystin-2 (PC2), transient receptor potential vanilloid channel 4 (TRPV4) or Piezo channels 1 and 2 have been shown to localise within the ciliary membrane and are postulated as signal transducers sensitive to mechanical alterations [2, 3, 13–20]. In kidney epithelial cells, bending of the cilium due to fluid flow was shown to result in an intracellular increase in calcium mediated by the extracellular levels of calcium itself [13, 14], while chondrocyte cilia respond to compression through a purinergic calcium signalling pathway [21, 22]. However, recent research showed that the cytoplasmic calcium waves observed in cells following flow-induced ciliary bending were initiated away from primary cilia [23, 24], thus contradicting the conventional hypothesis that calcium influx into cilium is responsible for triggering this response.

The incongruence on present data is partially caused by the difficulties associated with studying electrophysiology of primary cilia. The narrow diameter of the cilium (typically around 250 nm) approaches the resolution limit of conventional optical microscopy limiting its use for navigating microelectrodes. To date, few studies have been able to obtain direct electrophysiological recordings from optically identifiable parts of cilia [1, 19, 25]. Given the heterogenous distribution of membrane strain during bending [26], novel approaches capable of mapping channel and receptor sensitivity to external stimuli along the cilium are needed.

Here we employ scanning ion conductance microscopy (SICM), a scanning probe microscopy technique that uses a glass nanopipette as a probe to scan the surface of living cells in a non-contact fashion to obtain topographical images with nanoscale resolution [27, 28]. The high resolution topographical information obtained using SICM has been previously combined with patch-clamp to obtain single channel recordings from specific cellular structures below the resolution limit of conventional optically based positioning such as T-tubules or small synaptic boutons [1, 29, 30]. Recently, the hopping mode of SICM has been successfully used to image fixed primary cilia [31], however, spatially resolved single channel recordings in live cilia under mechanical stimulation have not been achieved yet.

Materials and Methods

Inner medullary collecting duct (IMCD) cell culture

Mouse IMCD epithelial cells from an immortalised line genetically modified to express enhanced yellow fluorescent protein together with intraflagellar transport protein 88 (IFT88-YFP [32, 33]) were cultured at 37°C and 5% CO_2 in Dulbecco's modified Eagle medium (DMEM) with a supplement of 10% of foetal bovine serum (v/v), 1.9mM L-glutamine, 96U/mL penicillin and 96mg/mL streptomycin. Cells were cultured until confluence and then either used for experimentation or passaged for up to passage number 25. To obtain high levels of ciliation for experiments, IMCD cells were cultured in 35mm petri dishes to ~100% confluence and then serum starved (0.2% FBS) for 24-72 hours.

High-resolution scanning of primary cilia

Topographical images were obtained using hopping mode of the SICM (also known as HIPCM) using a custom-built SICM scanner head operated by SICM scanner controller (Ionscope Ltd, UK) and a custom-built

software described previously [28, 34]. Axopatch 200B (Molecular Devices) was used for nanopipette current measurement. The SICM scan head was positioned onto an inverted optical microscope (Eclipse TE300, Nikon) placed on an anti-vibration table (PFA51507, Thorlabs). Setpoint of 0.3% was used for imaging. Once putative primary cilia were identified in topographical images, YFP-positive fluorescence imaging (Zeiss 710 ELYRA PS.1, Carl Zeiss) was used to confirm identity. A non-invasive low-stress method described previously [35] was used to obtain stiffness maps of primary cilia. Briefly, two sets of topographical images of the same area were simultaneously recorded at two different setpoints: 0.3% (estimated compressive force 0.003 pN) and 1% (estimated compressive force of 0.225 pN). The difference between the two images was used to obtain the information on displacement at each imaging point and calculate stiffness. Nanopipettes were pulled from borosilicate glass (OD 1mm, ID 0.5mm, Sutter Instruments, USA) using laser puller P-2000 (Sutter Instruments, USA). Nanopipettes resistance was ~70-110 MΩ, corresponding to an estimated inner tip diameter ~90-125nm.

Mapping mechanosensitivity of membrane channels

Once a high-resolution topographical image was obtained, the specific coordinates of the primary cilium were used for precise positioning the nanopipette on the cilium, using approach referred to as "smart-patch-clamp" [29]. Light suction (~10 kPa) was used to obtain the gigaohm seal. Single-channel currents were amplified using Axopatch200B (Axon Instruments, USA), filtered at 1 kHz, and digitised at 200 kHz using data-acquisition system NI USB-6341 (National Instruments, USA) and WinEDR V3.7.1 software (John Dempster, University of Strathclyde). Mechanosensitivity of single-channels was assessed by gradually changing the vertical position of the pipette upwards and downwards in steps of 100 nm or by suction applications (pressure clamps) of ~20 to 50 kPa, all while keeping the nanopipette potential at V_H = -140 mV. The order of z-axis displacement was randomly tested for each recording, going either firstly upwards, then returning to 0 nm displacement, and then continuing downwards or the other way round. Stimulation in the opposite z-direction was only tested when recoding at 0 nm displacement showed similarity, reversibility, as baseline conditions. All potentials in the single-channel data presented here are nanopipette potentials.

Nanopipette and bath solutions

Cells were imaged in phenol red-free Leibovitz's L-15 medium (Gibco) at room temperature. Nanopipettes were filled with saline solution (0.154 mol/L of NaCl at pH = 7.4). In experiments aimed at testing sensitivity of channels to ATP, 10μM ATP (Sigma) was added to the nanopipette saline solution. To confirm the origin of activity induced by membrane displacement, 10μM $GdCl_3$ (Sigma), a nonspecific blocker of cation and mechanosensitive channels, was added to the nanopipette saline solution.

Statistical methods

GraphPad Prism (version 7 for Windows) was used for all statistical analysis. Un/paired t-test, or multiple t-test using the Holm-Sidak method, was used to statistically analyse differences in elastic modulus, bending stiffness, open probability (P_o) and mean open time (MOT). To statistically assess the differences in slope conductance, a two-tailed analysis of covariance (ANCOVA) was used. Differences were regarded as significant at p-values smaller than 0.05 (α=5%). Data are described as mean ± standard error mean (SEM).

Results

Topography-guided recording of membrane channel activity in primary cilia

To confirm the identity of live primary cilia and their presence at the apical membrane accessible to the scanning nanopipette, we used IMCD epithelial cell line which stably express intraflagellar transport protein IFT88 labelled with yellow fluorescence protein (IFT88-YFP) and correlated the high-resolution topography obtained using SICM with epifluorescence microscopy images of the same area (Fig. 1A-C). A total of 65 cilia were identified and successfully scanned. Primary cilia were situated peri-centrally within the apical (lumen) side of the cells and showed an average total length of 1.51 ± 0.074 μm (mean ± SEM).

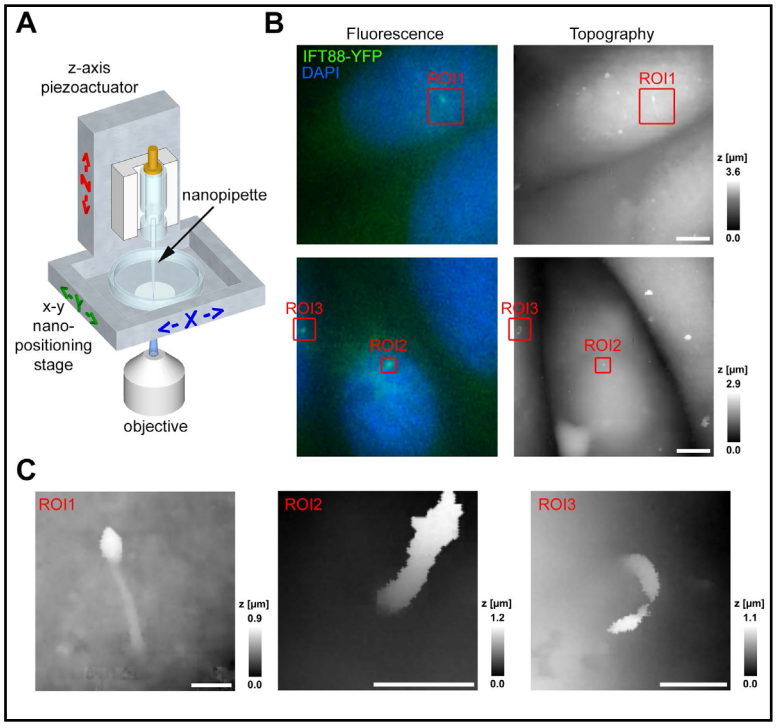

Fig. 1. Identification of primary cilia in IMCD IFT88-YFP epithelial cells using hopping mode SICM and epifluorescence. Schematic of the SICM setup mounted on top of epifluorescence microscope (A). Epifluorescence (B, left) and height-coded SICM topography images (B, right) of the same area of fixed (4% paraformaldehyde) kidney epithelial cells showing the fluorescent cilia in green (IFT88 labelled with YFP) and the nucleus with DAPI (1µg/ml). High-resolution topography of primary cilia (C) identified in the individual regions of interest ROI1-ROI3 marked in (B). Scale bars 5 µm (B), 1 µm (C).

The digital coordinates from the 3D images were used to position the scanning pipette at selected points on cilia (tip, middle part and base) and extra-ciliary membrane (ExC) and perform single-channel recordings at these positions (Fig. 2A). Overall, the success rate of obtaining cell-attached patch-clamp configuration was 70.77 % (46 out of 65). The success rate was highest at the base of cilia (75 %, 18 out of 24), followed by the extra-ciliary membrane (66.6 %, 8 out of 12) and the tip of the cilium (65.21 %, 15 out of 23), while the middle part of cilia was the most difficult area to record from (success rate 37.5 %, 3 out of 8). At the base of cilia, channels were recorded in 15 out of 18 successful patches (83.33 %), displaying mean slope conductance of 41.87 ± 2.252 pS (R^2 = 0.9376, n = 9) and a current reversing point at -13.03 mV (Fig. 2B, C). At the tip of the cilia, channel activity was detected in 60% of cases (9 out of 15) with a mean slope conductance of 23.39 ± 1.936 pS (R^2 = 0.869, n = 6) and a current reversing point at -0.46 mV (Fig. 2B, C). Within the randomly selected ExC areas, 75% (6 out of 8) of the successful patches showed channel activity. Assuming circular shape of the patch area and average inner diameter of nanopipettes d = 108 nm (range of 90-125 nm), the average patch area would be

$$\pi \times \left(\frac{d}{2}\right)^2 = 0.009 \mu m^2.$$

With 60 – 80 % of patches on cilia showing channel activity, the estimated channel density would be 6 - 8 channels per 0.09 µm² or 67 - 88 channels per µm².

The population of channels outside cilia appeared to be more heterogeneous than that observed within the ciliary membrane as indicated by relatively low R^2 of the linear regression of current-voltage dependence yielding mean slope conductance of 67.67 ± 13.16 pS (R^2 = 0.5821, n = 5, Fig. 2B, C). The channels in these patches showed a current reversing point at 2.686 mV. Due to low success rate of forming cell-attached configuration at the middle part of the cilia, we were not able to obtain reliable current-voltage dependency of channels present at this location. The mean resting membrane potential of the cells measured using conventional zero-current clamp whole-cell patch clamp configuration was -32.4 ± 1.6 mV (mean ± SEM, n = 7).

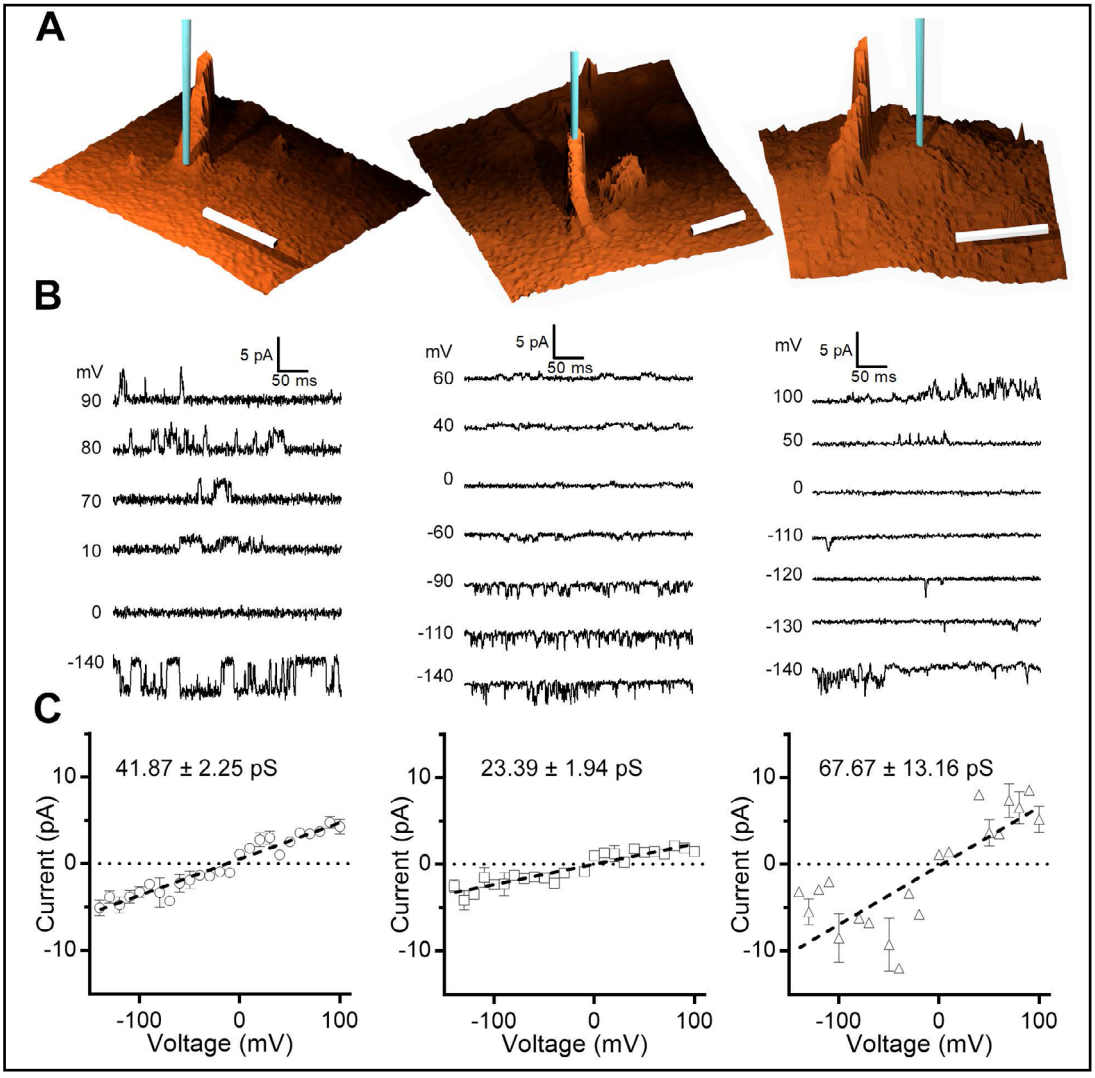

Fig. 2. Spatially resolved ion-channel recordings in primary cilia. Representative 3D topographical images of primary cilia (A) illustrating positioning of nanopipette (shown in blue) at the base of a cilium (left), tip (middle) and extra-ciliary membrane (right) to perform recordings. Scale bars 1 µm. Representative single-channel currents (B) recorded from the base of primary cilia (left), tip of cilia (middle), and extra-ciliary membrane (right). I/V curves of average (±SEM) single-channel current amplitudes (C) recorded at the base (left, n = 9), tip of cilia (middle, n = 6), and extra-ciliary membrane (right, n = 7). Voltages shown are nanopipette potentials against the ground electrode in the bath. All recordings shown were performed in the cell-attached mode.

Statistical analysis showed that differences between the slope conductance of channels observed at the three locations were all significant indicating heterogeneous distribution of ion channels within ciliary membrane as well as between ciliary and extra-ciliary membrane (ANCOVA; base vs tip $p < 0.001$, $F = 38.56$, $DFn = 1$; base vs ExC $p = 0.0468$, $F = 4.198$, $DFn = 1$; tip vs ExC $p = 0.0012$, $F = 12.19$, $DFn = 1$).

Mapping mechano-sensitivity of ion channels in primary cilia

To investigate whether the ion channels observed in cilia could be involved in mechanotransduction we applied local mechanical stimulations at various locations along the primary cilium, and the cell body by means of applying negative pressure through the scanning nanopipette and by changing the z-axis position of the nanopipette in steps of

100 nm (Fig. 3), while recording the single channel activity. While the application of suction did not induce any detectable channel activity (data not shown), moving the nanopipette along the z-axis induced significant changes in mean open probability P_o of ion channels at the base of cilia (Fig. 3A). Z-axis displacement of +100 nm (upwards) induced a significant increase in the normalised P_o of channels at the base of cilia (unpaired t-test, n = 4, p = 0.0221, t = 4.377, df = 3; Fig. 3A). Negative -100 nm displacement (downwards) also led to increase in normalised P_o of the channels at the base of cilia, although not statistically significant (n = 4, p = 0.0564, t = 3.028, df = 3; Fig. 3A). In stark contrast, the open probability of channels at the tip of cilia (Fig. 3B) significantly decreased upon both the positive and negative displacements (at +100nm, n = 3, p = 0.0466, t = 13.64, df = 2; at -100nm, n = 2, p = 0.0036, t = 174.9, df = 1). Similar to the ciliary tip, the open probability of channels on the extra-ciliary membrane decreased significantly at -100nm (n = 3, p = 0.0025, t=253.7, df = 2) but insignificantly at +100nm (n = 4, p = 0.1207, t = 2.611, df = 3). There was no further significant change in open probability when displacing more than 100 nm in any cases, when compared to the 100 nm displacement.

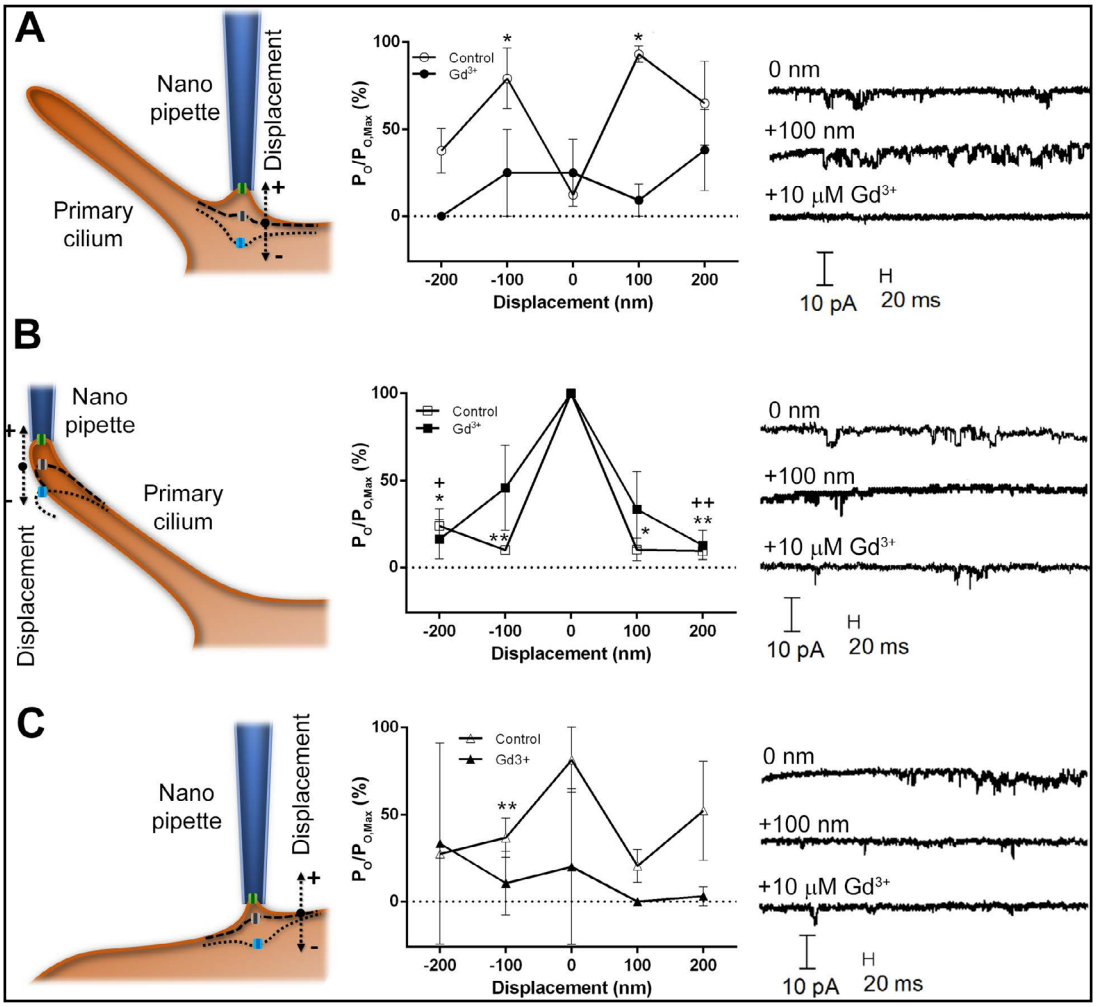

Fig. 3. Mapping mechano-sensitivity of ion channels at cilia base (A), cilia tip (B) and extra-ciliary regions (C). The left panels illustrate the displacement, the middle panels show the effect of the displacement on the mean normalised open probability P_o of channels at pipette potential of -140 mV, and the right panels show example single-channel recordings. All values are shown as mean ± S.E.M (n=5 at cilia base, n = 3 at cilia tip, n = 5 at extra-ciliary regions. Significant differences with respect to zero displacement under control conditions (absence of Gd^{3+}) are marked as *p<0.05 and ** p<0.01 (open symbols). Significant differences with respect to zero displacement in presence of Gd^{3+} are shown as $^{+}$p<0.05 and $^{++}$p<0.01 (closed symbols).

No statistically significant changes in the open probability of channels at the base of cilia and extra-ciliary membrane were observed when the displacement was performed in presence of 10 µM Gd^{3+} (a nonspecific blocker of cation and mechanosensitive channels [36, 37]) applied through the scanning nanopipette (base, n = 5, p = 0.1909; ExC, n = 5, p = 0.062 Fig. 3A, C). Interestingly, a significant decrease in the open probability of channels at the tip of cilia upon ± 200 nm displacement was observed even in presence of 10 µM Gd^{3+} (at + 200 nm, n = 3, p = 0.0018, t=23.82, df = 2; at - 200 nm, n = 3, p = 0.0213, t = 6.745, df = 2, Fig. 3C).

Mapping channel sensitivity to ATP

It has been previously suggested that mechanotransduction could be mediated via ATP-sensitive channels and receptors [1, 9, 21, 22]. To map the sensitivity of channel activity in primary cilia to ATP we performed spatially resolved recordings at the three sites (tip and base of cilia, and extra-ciliary membrane) with 10 µM ATP in the scanning nanopipette (Fig. 4). The presence of ATP in the nanopipette significantly increased the open probability P_o of the channels at the base of cilia (n = 5; paired t test, p = 0.0146, t = 3.0131, df = 9) but not at the tip of cilia (n = 4; paired t test, p = 0.4073, t = 0.8909, df = 6) or outside the cilia (n = 6; paired t test, p = 0.0657, t = 2.1305, df = 8).

Mapping stiffness of primary cilia

To explore possible reasons for the observed differences in mechanosensitivity of the channels at the base and the tip of cilia, we looked into mechanical properties of these two sites. We utilised the capability of the SICM to map elastic modulus simultaneously with topography at very low stress and high resolution (Fig. 5) [35]. The mapping showed that stiffness at the tip of the cilia (0.49 ± 0.09 pN/µm, n = 7) was significantly lower than both the stiffness at the base (2.75 ± 0.45 pN/µm, n = 7, paired t-test, p = 0.0012, t = 5.78, df = 6) and outside cilia (3.9 ± 1.071 pN/µm, n = 7, p = 0.016, t = 3.33, df = 6) (Fig. 5B). However, the stiffness at the base of cilia was not significantly different from the extra-ciliary membrane (p = 0.255, t = 1.26, df = 6) (Fig. 5B). We would like to stress here that unlike in the experiments focused on mechanosensitivity of single channels (Fig. 3), the measurement of stiffness is a non-contact measurement (Fig. 5A), which means we have direct control over the direction of displacement of the nanopipette but not the structure being probed. Therefore, we cannot exclude the possibility that the moveable parts of cilia (particularly the middle and the tip) may be displaced sideways in addition to or instead of downwards while measuring stiffness (Fig. 5A).

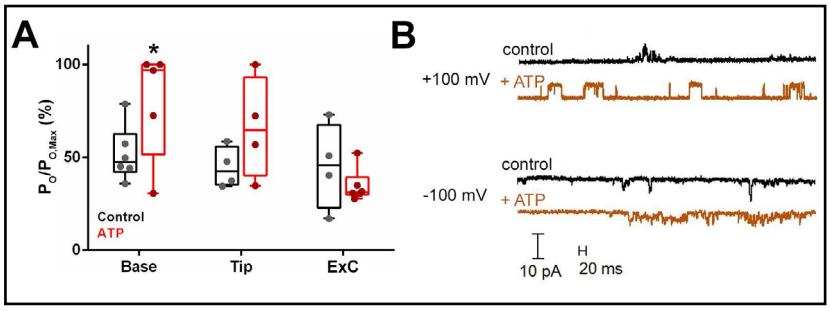

Fig. 4. Effect of ATP on spatially resolved single-channel recordings in primary cilia. (A) Normalised mean open probability P_0 of channels in control (black symbols) and presence of 10µM ATP in the pipette solution (red symbols) at the base of cilia, the tip of cilia, and at randomly selected areas of the extra-ciliary membrane (ExC). (B) Representative excerpts of single-channel activity at pipette potentials of 100mV and -100mV recorded at the base of a cilium in control conditions (black) and in presence of ATP (orange). * p<0.05. Voltages shown are nanopipette potentials against the ground electrode. All recordings are in the cell-attached configuration.

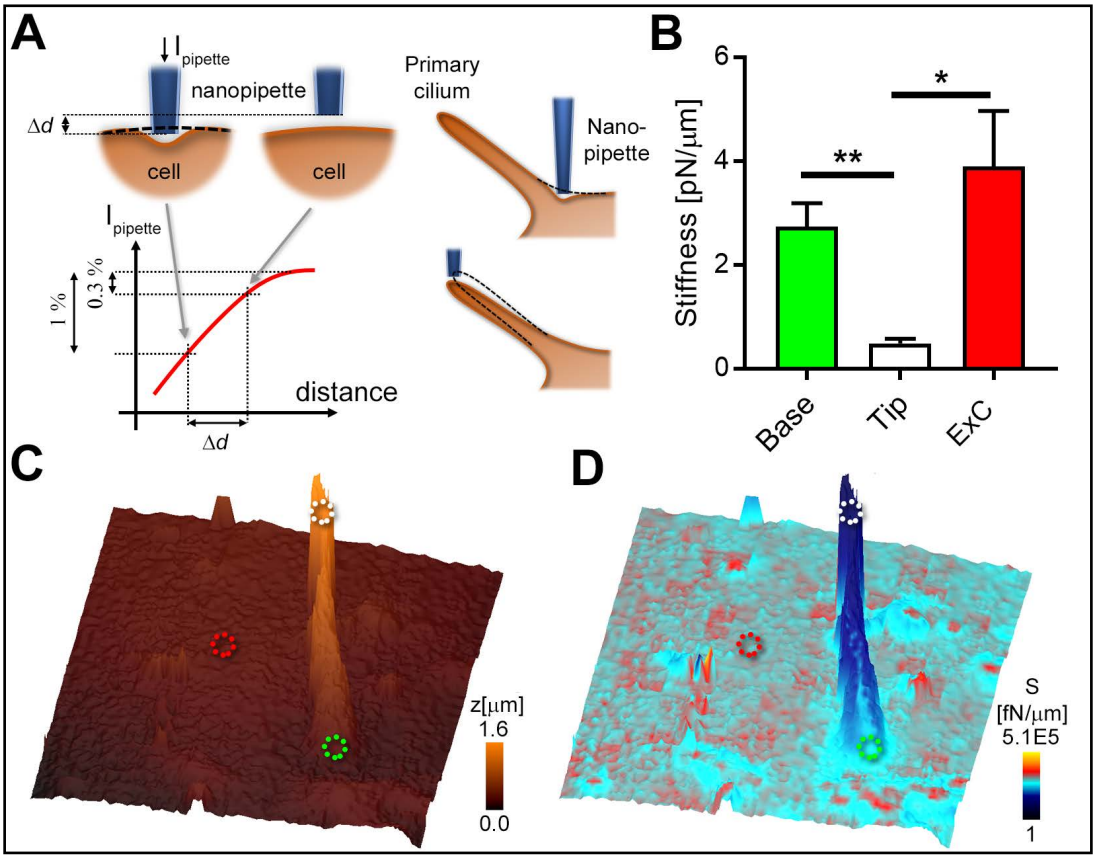

Fig. 5. Mapping stiffness of primary cilia. (A) Principle of non-contact measurement of stiffness using SICM. Displacement between 0.3 % current drop (typical topography setpoint) and 1% current drop is measured to obtain the stiffness. As illustrated on the right, the measurement is likely to cause compression in extra-ciliary membrane as well as at the base of cilia, but more likely to cause pivoting or bending of the whole cilium when targeting the tip of cilia. (B) Comparison of mean stiffness of cilia base and tip versus extra-ciliary membrane (ExC) (n = 7). Example of simultaneously obtained height-coded topography image of a live primary cilium (C) and its stiffness map (D). The dotted circles mark the membrane regions of cilium tip (white), cilium base (green) and extra-ciliary membrane (red). *p<0.05, **p<0.01

Discussion

Here, we describe a novel strategy for studying ion channel distribution in primary cilia along with their mechanical and chemical sensitivity at nanoscale resolution. Spatial resolution of previous single-channel cell-attached recordings in primary cilia was limited by the use of optical navigation [1, 19, 25, 38] incapable of resolving the ultrastructure of primary cilium and the recordings typically involved suction of the cilia towards or into the nearby recording pipette possibly causing unknown levels of displacement and mechanical strain to the structure of cilium. Our recordings here show that displacements as small as 100 nm can significantly affect channel activity in primary cilia.

Primary cilia in topographical images obtained using SICM in this study are somewhat shorter than reported in previous studies using fluorescence measurements [32], but still within the range of cilia from normal non-cultured renal tubular cells [13]. Topographical images only reveal the part of the cilium extending into the extracellular space which may be shorter than the actual axoneme of the cilium if the ciliary structure does not completely migrate to the surface level [10, 39]. This further emphasises the importance of using topographical images for precise positioning of recording nanopipette to parts of cilia

other than the tip such as the middle and base which cannot be determined just from the fluorescence image alone.

Our single-channel recordings suggest ciliary channel density of 67-88 channels per μm^2 which is somewhat lower than the previously reported 128 channels per μm^2 estimated from whole-cilium currents [1], but is in agreement with the general idea of ciliary channel density being comparable to that of excitable plasma membranes [1]. We observed differences in both the slope conductance and mechanosensitivity of channels recorded at different positions along the accessible structure of cilia. Channels detected at the tip of cilia in our experiments displayed slope conductance corresponding to endogenous channels in primary cilia of IMCD cells when using NaCl-based pipette solution [40]. Despite these differences in conductance, channels at the tip and the base of the cilia as well as outside of cilia were blocked by Gd^{3+} and activated by ATP in agreement with previous reports [1]. Heterogeneous distribution of channels throughout the membrane of cilia has been previously suggested based on either immunoflurescent staining or channel recordings in larger olfactory cilia [2, 3,13–18], however direct experimental evidence in smaller cilia as reported here was missing. The importance of using direct recording to prove functionality of channels has been recently demonstrated in a study reporting that PC2 forms functioning ion channel in primary cilia of kidney cells but has no measurable constitutive activity in the plasma membrane, which, as the authors themselves note, could not be ruled out based on fluorescence study only [19]. The differences in slope conductance we observed here may therefore be a result of the different environment faced by the channels at tested location or by channels being assembled from different subunits, as previously demonstrated in transiently transfected HEK293 cells [1].

Perhaps the most interesting finding in our study is the effect of vertical displacement on channel activity at the base and at the tip of the cilia. A short cilium is expected to behave as a rigid rod pivoting around a hinge below the basal body for the displacements of few hundred nanometres used here [41]. The different response of channels to vertical displacement at the tip (reduction of open probability) compared to the base (increase in open probability) may be caused by the differences in the underlying structure of the two locations which would ultimately result in different distribution of mechanical strain. The base of cilium with its underlying structure comprising of transition fibres, basal body and anchorage to actin cytoskeleton is significantly more complex than the structure at the tip. Small displacement of the nanopipette sealed to the tip of cilia is most likely to transpose into pivoting of the whole cilium while displacement of the nanopipette at the base is likely to mainly strain the membrane anchored to transition fibres and the actin cytoskeleton. This is also reflected in our measurements of stiffness which show the tip of cilium as apparently softer than the base. Previous models also suggested that mechanical strain in a bending cilium is likely to be highest at the base [26]. It has been hypothesised that the channels at the base could be triggered by pivoting prevailing at lower external forces while channels along the length of the cilium could be triggered by cilium bending which requires higher forces [41]. Channels at the base of cilia could be acting as a "gating spring" triggered via their anchoring to the actin cytoskeleton [42–45]. Our results lend some support to these hypotheses, providing first direct experimental evidence for heterogeneous mechanosensitivity of ion channels along the structure of cilia.

The channel activity at the base and the tip of the cilia recorded here was sensitive to Gd^{3+}, a commonly used non-specific blocker of mechanotransduction [36], and ATP in a similar fashion to PC1/PC2 channels reported previously [1, 9,14, 21, 22], but we did not observe changes in channel activity upon application of negative pressure. This may be due to the fact that the force exerted on the membrane patch enclosed within the tip of a nanopipette with 100 nm inner diameter is expected to be two orders of magnitude lower than in case of conventional patch-clamp pipette with tip diameter of 1 μm when using the same pipette pressure, simply due to membrane patch area being proportional to the square of the pipette radius. In order to reach forces exerted previously using 80 mm Hg ~ 11 kPa [1], we would have to apply 1.1 MPa which is prohibitively high. While this certainly limits

the capabilities of nanopipettes for testing channels activated specifically by membrane stretch, nevertheless, mechanical stimulation via vertical displacement used here appears to be more relevant to what membrane channels may experience during the pivoting and bending of cilia under external forces.

The channel activity we observed in cilia was markedly different compared to channel activity recorded on the extra-ciliary membrane. It displayed significantly different mean slope conductance and lacked the strong sensitivity to displacement. This lends further experimental support to previous observations and hypotheses that the population of channels in primary cilia is different to that of the cytoplasmic membrane [2, 3,13–16, 18]. Furthermore, the markedly different character of the response to nanopipette displacement in the extra-ciliary membrane, together with Gd^{3+} sensitivity of the response observed in cilia base indicates these changes are unlikely to be caused simply by deterioration of the seal between the nanopipette during the displacements and represent genuine changes in channel activity.

Conclusion

In summary, we show the first channel recordings at defined positions along primary cilia using high resolution topographical imaging and local and precisely controlled mechanical stimulation. Our data suggest that ion channels at the base of cilia in IMCD cells are activated by membrane displacement and ATP and may play a role in mechanotransduction. These recordings would have been extremely difficult if not impossible to achieve using pipette navigation based on conventional fluorescence-based imaging of cilia due to the fact that some parts of cilia could be still submerged within intracellular space. Furthermore, significant changes in open probability were induced by mere 100 nm displacement of the cilia membrane suggesting nanoscale positioning is essential to minimise unwanted mechanical strain when studying mechanotransduction in these fine structures.

The method described here opens new possibilities to study relationship between the structure of primary cilia and its function in health and disease, and could serve as a tool for screening new compounds specifically targeting channels and receptors in primary cilia. Future research combining the technology described here with genetics strategies, such as small interfering RNA (siRNA) to selectively modify expression of putative channels, and local applications of specific agonist and antagonists through nanopipette will be crucial to determine which functions could be directly attributed to primary cilia.

Acknowledgements

Statement of Ethics
The authors have no ethical conflicts to disclose.

Funding Sources
This study was funded by the Wellcome Trust (Seed Award in Science, 109724/Z/15/Z to P.N.) and received financial support from the Ministry of Education and Science of the Russian Federation in the framework of increase Competitiveness Program of NUST ‘‘MISIS”, implemented by a governmental decree dated 16th of March 2013, No 211.

Author Contributions
J.T.P. performed imaging and electrophysiological experiments, analysed the data and wrote the manuscript. H.N. performed stiffness mapping of primary cilia. C.L.T. participated in experiment preparations and manuscript writing. M.M.K. helped to conceive and design the research. P.N. conceived and designed the research, performed data analysis and manuscript writing. All authors discussed the results and commented on the manuscript.

Disclosure Statement

The authors have no conflicts of interest to declare.

References

1 Decaen PG, Delling M, Vien TN, Clapham DE: Direct recording and molecular identification of the calcium channel of primary cilia. Nature 2013;504:315–318.
2 Eichholz KF, Hoey DA: The Role of the Primary Cilium in Cellular Mechanotransduction, in Simon RC (ed): Mechanobiology: Exploitation for Medical Benefit. John Wiley & Sons, Inc., 2016, pp 61–73.
3 Nauli SM, Sherpa RT, Reese CJ, Nauli AM: Mechanosensory and Chemosensory Primary Cilia in Ciliopathy and Ciliotherapy, in Simon RC (ed): Mechanobiology: Exploitation for Medical Benefit. John Wiley & Sons, Inc., 2016, pp 75–99.
4 Pablo JL, DeCaen PG, Clapham DE: Progress in ciliary ion channel physiology. J Gen Physiol 2016;149:37–47.
5 Christensen S, Pedersen L, Schneider L, Satir P: Sensory cilia and integration of signal transduction in human health and disease. Traffic 2007;8:97–109.
6 Singla V, Reiter JF: The primary cilium as the cell's antenna: signaling at a sensory organelle. Science 2006;313:629–633.
7 Takacs Z, Proikas-Cezanne T: Primary cilia mechanosensing triggers autophagy-regulated cell volume control. Nat Cell Biol 2016;18:591–592.
8 Tobin JL, Beales PL: The nonmotile ciliopathies. Genet Med 2009;11:386–402.
9 Alaiwi WAA, Lo ST, Nauli SM: Primary cilia: Highly sophisticated biological sensors. Sensors 2009;9:7003–7020.
10 Benmerah A: The ciliary pocket. Curr Opin Cell Biol 2013;25:78–84.
11 Szymanska K, Johnson C: The transition zone: an essential functional compartment of cilia. Cilia 2012;1:10.
12 Ishikawa H, Marshall WF: Mechanobiology of Ciliogenesis. Bioscience 2014;64:1084–1091.
13 Praetorius HA, Spring KR: Bending the MDCK Cell Primary Cilium Increases Intracellular Calcium. J Membr Biol 2001;184:71–79.
14 Nauli SM, Alenghat FJ, Luo Y, Williams E, Vassilev P, Li X,Elia AE, Lu W, Brown EM, Quinn Sj, Ingber DE, Zhou J: Polycystins 1 and 2 mediate mechanosensation in the primary cilium of kidney cells. Nat Genet 2003;33:129–137.
15 Kim S, Nie H, Nesin V, Tran U, Outeda P, Bai CX, Keeling J, Maskey D, Watnick T, Wessely O , Tsiokas L: The polycystin complex mediates Wnt/Ca2+ signalling. Nat Cell Biol 2016;18:752-764.
16 O'Conor CJ, Leddy H a, Benefield HC, Liedtke WB, Guilak F: TRPV4-mediated mechanotransduction regulates the metabolic response of chondrocytes to dynamic loading. Proc Natl Acad Sci U S A 2014;111:1316–1321.
17 Nechipurenko I V, Doroquez DB, Sengupta P: Primary cilia and dendritic spines: different but similar signaling compartments. Mol Cells 2013;36:288–303.
18 French DA, Badamdorj D, Kleene SJ: Spatial distribution of calcium-gated chloride channels in olfactory cilia. PLoS One 2010;5:e15676.
19 Liu X, Vien T, Duan J, Sheu S, Decaen PG, David E: Polycystin-2 is an essential ion channel subunit in the primary cilium of the renal collecting duct epithelium. Elife 2018;1–30.
20 Wang Z, Ng C, Liu X, Wang Y, Li B, Kashyap P, Chaudhry HA, Castro A, Kalontar EM, Ilyayev L, Walker R, Alexander RT, Qian F, Chen XZ, Yu Y: The ion channel function of polycystin-1 in the polycystin-1/polycystin-2 complex. EMBO Rep 2019;1–18.
21 Rodat-Despoix L, Hao J, Dandonneau M, Delmas P: Shear stress-induced Ca^{2+} mobilization in MDCK cells is ATP dependent, no matter the primary cilium. Cell Calcium 2013;53:327–337.
22 Wann A, Zuo N, Haycraft C, Jensen C: Primary cilia mediate mechanotransduction through control of ATP-induced Ca2+ signaling in compressed chondrocytes. FASEB J 2012;26:1663–1671.
23 Delling M, Indzhykulian AA, Liu X, Li Y, Xie T, Corey DP, Clapham DE: Primary cilia are not calcium-responsive mechanosensors. Nature 2016;531:656-660.

24 Norris DP, Jackson PK: Cell biology: Calcium contradictions in cilia. Nature 2016;531:582–583.
25 Kleene NK, Kleene SJ: A method for measuring electrical signals in a primary cilium. Cilia 2012;1:1.
26 Mathieu PS, Bodle JC, Loboa EG: Primary cilium mechanotransduction of tensile strain in 3D culture: Finite element analyses of strain amplification caused by tensile strain applied to a primary cilium embedded in a collagen matrix. J Biomech 2014;47:2211–2217.
27 Hansma PK, Drake B, Marti O, Gould SA, Prater CB: The scanning ion-conductance microscope. Science 1989;243:641–643.
28 Novak P, Li C, Shevchuk AI, Stepanyan R, Caldwell M, Hughes S, Smart TG, Gorelik J, Ostanin VP, Lab MJ, Moss GW, Frolenkov GI, Klenerman D, Korchev YE: Nanoscale live-cell imaging using hopping probe ion conductance microscopy. Nat Methods 2009;6:279–281.
29 Novak P, Gorelik J, Vivekananda U, Shevchuk AII, Ermolyuk YSS, Bailey RJ, Bushby AJ, Moss GW, Rusakov DA, Klenerman D, Kullmann DM, Volynski KE, Korchev YE: Nanoscale-Targeted Patch-Clamp Recordings of Functional Presynaptic Ion Channels. Neuron 2013;79:1067–1077.
30 Gorelik J, Gu Y, Spohr H a, Shevchuk AI, Lab MJ, Harding SE, Edwards Cr, Whitaker M, Moss GW, Benton DC, Sánchez D, Darszon A, Vodyanov I, Klenerman D, Korchev YE: Ion channels in small cells and subcellular structures can be studied with a smart patch-clamp system. Biophys J 2002;83:3296–3303.
31 Zhou Y, Saito M, Miyamoto T, Novak P, Shevchuk AI, Korchev YE, Fukuma T, Takahasi Y: Nanoscale Imaging of Primary Cilia with Scanning Ion Conductance Microscopy. Anal Chem 2018;90:2891–2895.
32 Besschetnova TY, Roy B, Shah JV: Chapter 16 - Imaging Intraflagellar Transport in Mammalian Primary Cilia, in King SM, Pazour G (eds): Methods in Cell Biology. Academic Press 2009, pp 331–346.
33 Tran P V, Haycraft CJ, Besschetnova TY, Turbe-Doan A, Stottmann RW, Herron BJ, Chesebro AL, Qiu H, Scherz PJ, Shah JV, Yoder BK, Beier DR: THM1 negatively modulates mouse sonic hedgehog signal transduction and affects retrograde intraflagellar transport in cilia. Nat Genet 2008;40:403.
34 Novak P, Shevchuk A, Ruenraroengsak P, Miragoli M, Thorley AJ, Klenerman D, Lab MJ, Tetley TD, Gorelik J, Korchev YE: Imaging Single Nanoparticle Interactions with Human Lung Cells Using Fast Ion Conductance Microscopy. Nano Lett 2014;14:1202–1207.
35 Clarke RW, Novak P, Zhukov A, Tyler EJ, Cano-Jaimez M, Drews A, Richards O, Volynski K, Bishop C, Klenerman D: Low Stress Ion Conductance Microscopy of Sub-Cellular Stiffness. Soft Matter 2016;12:7953–7958.
36 Yang XC, Sachs F: Block of stretch-activated ion channels in xenopus oocytes by gadolinium and calcium ions. Science 1989;243:1068–1071.
37 Oliet SHR, Bourque CW: Gadolinium uncouples mechanical detection and osmoreceptor potential in supraoptic neurons. Neuron 1996;16:175–181.
38 Carrisoza-Gaytán R, Wang L, Schreck C, Kleyman TR, Wang WH, Satlin LM: The mechanosensitive BKα/β1 channel localizes to cilia of principal cells in rabbit cortical collecting duct (CCD). Am J Physiol Renal Physiol 2017;312:F143–156.
39 Mukhopadhyay S, Badgandi HB, Hwang S, Somatilaka B, Shimada IS, Pal K: Trafficking to the primary cilium membrane. Mol Biol Cell 2017;28:233–239.
40 Luo Y, Vassilev PM, Li X, Kawanabe Y, Zhou J: Native polycystin 2 functions as a plasma membrane Ca2+-permeable cation channel in renal epithelia. Mol Cell Biol 2003;23:2600–2607.
41 Battle C, Ott CM, Burnette DT, Lippincott-Schwartz J, Schmidt CF: Intracellular and extracellular forces drive primary cilia movement. Proc Natl Acad Sci 2015;112:1410–1415.
42 Janmey PA, McCulloch CA: Cell Mechanics: Integrating Cell Responses to Mechanical Stimuli. Annu Rev Biomed Eng 2007;9:1–34.
43 Howard J, Hudspeth AJ: Compliance of the hair bundle associated with gating of mechanoelectrical transduction channels in the Bullfrog's saccular hair cell. Neuron 1988;1:189–199.
44 Liu W, Xu S, Woda C, Kim P, Weinbaum S, Satlin LM: Effect of flow and stretch on the [Ca2+]i response of principal and intercalated cells in cortical collecting duct. Am J Physiol Ren Physiol Am J Physiol Renal Physiol 2003;285:998–1012.
45 Schwartz EA, Leonard ML, Bizios R, Bowser SS: Analysis and modeling of the primary cilium bending response to fluid shear. Am J Physiol Physiol 1997;272:F132–138.